A Measurement of the B^0 Lifetime

using Partial Reconstructed Hadronic B^0 Decays

including 1994 Data

Thorsten Oest, CERN

Abstract

B^0 mesons were reconstructed using two pions $\pi_B^+ \pi_D^-$ from a decay $B^0 \to \pi_B^+ D^{*-} X$ with $D^{*-} \to \pi_D^- \overline{D}^0$. 166 ± 13 B^0 were found in the 1991-1994 data. From this sample the B^0 lifetime was measured to be:

$$\tau_{B^0} = 1.50 \; {}^{+0.17}_{-0.15} \; {}^{+0.08}_{-0.06} \; ps.$$

1 Introduction

This analysis is an update including most of the 1994 data. In total $2,967,684$ class 16 events with VDET run selection for 1991-1993 were used. Requiring a primary vertex, found by QFNDIP, and high voltage in the TPC and VDET reduces the sample to $2,888,339$ events. Monte Carlo studies are based on the 1992,1993 HVFL Monte Carlo. In addition $7,848$ events with a decay $B^0 \to \pi^+(\rho^+)D^{*-} \to \pi^+(\rho^+)\pi^-\overline{D}^0$ and $10,066$ events of the type $B^+ \to \pi^+(\rho^+)D^{**0}$ were produced.

This analysis is essentially the same as described in the previous ALEPH note [1]. Therefore only a brief description of the analysis is given here. Two changes were made in respect to the old analysis:

- The minimization of χ^2_{dir}.
  The direction of the jet and the primary and secondary vertex position is combined to get the B^0 flight direction and decay length. The minimization procedure was improved resulting in a higher efficiency for small decay lengths.

- Tails in the resolution function for the decay length.
  The resolution function for the secondary vertex is parametrized with three gaussians (instead of two) to take into account tails in the distribution.

2 B^0 Selection

2.1 B^0 Reconstruction

B^0 decays

$$B^0 \to \pi_B^+ X \quad D^{*-} \\ \to \pi_D^- \overline{D}^0 \tag{1}$$

were reconstructed from two pions $\pi_B^+\pi_D^-$. The selection criteria are optimized to select $B^0 \to \pi^+(\rho^+)D^{*-}$ decays which contribute with $\approx 62\%$ to the final B^0 sample. The slow pion from the D^{*-} decay carries enough information on the D^{*-} momentum to allow a B^0 momentum reconstruction without seeing the D^0.

The B^0 three momentum is reconstructed in the $\pi_B^+\pi_D^-$ rest frame where the B^0 energy is given by:

$$E_B^* = \frac{M_B^2 + M_{\pi_B\pi_D}^2 - M_{XD^0}^2}{2M_{\pi_B\pi_D}} \tag{2}$$

The XD^0 mass is set to $M_{XD^0} = 2.1$ GeV. For decays where the true missing mass is close to this value the direction of the B^0 can be approximated by the direction of the slow pion:

$$\vec{p}_B^* \approx \sqrt{(E_B^*)^2 - M_B^2} \cdot \frac{\vec{p}_{\pi_D}^*}{|\vec{p}_{\pi_D}^*|} \tag{3}$$

The B^0 momentum in the laboratory frame is obtained after a retransformation. The angular resolution for a mixture of $B^0 \to \pi^+(\rho^+)D^{*-}$ decays is about 12 mrad. In

figure 1 the momentum resolution after all cuts for a full simulation of $B^0 \to \pi^+ X D^{*-}$ decays is displayed.

The $\pi_B^+ \pi_D^-$ mass will be used as signature for the B^0 decay. Due to kinematic reasons this mass cannot exceed 1.5 GeV. The lower bound is around 1 GeV for the decays $B^0 \to \pi^+(\rho^+)D^{*-}$.

2.2   Reconstruction of the Decay Length

The B^0 decay vertex is measured directly by the secondary vertex $\vec{r}_{\pi\pi}$ of the two pions. This position is not very well determined due to the slow pion from the D^{*-}. Therefore the jet direction $\vec{d}_{jet}$ was combined with the main vertex $\vec{r}_{main}$ from QFNDIP and the secondary vertex $\vec{r}_{\pi\pi}$ to get a better estiamtion for the B^0 decay length and flight direction $\vec{\ell}_B$. Minimizing

$$
\begin{aligned}
\chi^2_{dir} = {} & \left(\vec{r}_{main} - \vec{r}_B + \vec{\ell}_B\right)^T V^{-1}_{main} \left(\vec{r}_{main} - \vec{r}_B + \vec{\ell}_B\right) \\
& + \left(\vec{r}_{\pi\pi} - \vec{r}_B\right)^T V^{-1}_{\pi\pi} \left(\vec{r}_{\pi\pi} - \vec{r}_B\right) \\
& + \left(\vec{d}_{jet} - \vec{\ell}_B\right)^T V^{-1}_{jet} \left(\vec{d}_{jet} - \vec{\ell}_B\right)
\end{aligned}
\tag{4}
$$

gives the decay length and flight direction $\vec{\ell}_B$ and the B^0 decay position. The angular resolution of the jet direction is determined from Monte Carlo events:

$$
\begin{aligned}
\sigma_\beta(E_B/E_{jet}, \, \cos\vartheta_{jet}) &= \sigma_\phi(E_B/E_{jet}) \cdot f(\cos\vartheta_{jet}) \\
\sigma_\phi(E_B/E_{jet}) &= \left(0.039 - 0.029\frac{E_B}{E_{jet}}\right) \text{ mrad} \\
f(\vartheta_{jet}) &= 0.88 + 0.35 \, |\cos\vartheta_{jet}|
\end{aligned}
\tag{5}
$$

The resolution on the decay length obtained from the minimization procedure is shown in figure 1.

The decay time follows from the decay length $|\vec{\ell}_B|$ and the B^0 momentum:

$$
t = \frac{|\vec{\ell}_B| \cdot M_B}{|\vec{p}_B| \cdot c}
\tag{6}
$$

2.3   Data Selection

The selection starts with the reconstruction of pions.

- **The $\pi_B^+ \pi_D^-$ selection:**
  any track is defined as $\pi^\pm$ candidate if not identified as lepton or belonging to a V0 (KEFOTY = 0). In addition an existing dE/dx measurement with more than 50 measured points has to agree with the pion hypothesis within 3 standard deviations.

  Two charged pions $\pi_B^+ \pi_D^-$ are selected. A vertex fit is applied to get the B^0 decay vertex (YTOPOL). Pion combinations are accepted if $\chi^2_{\text{YTOPOL}}/NoF < 9$.
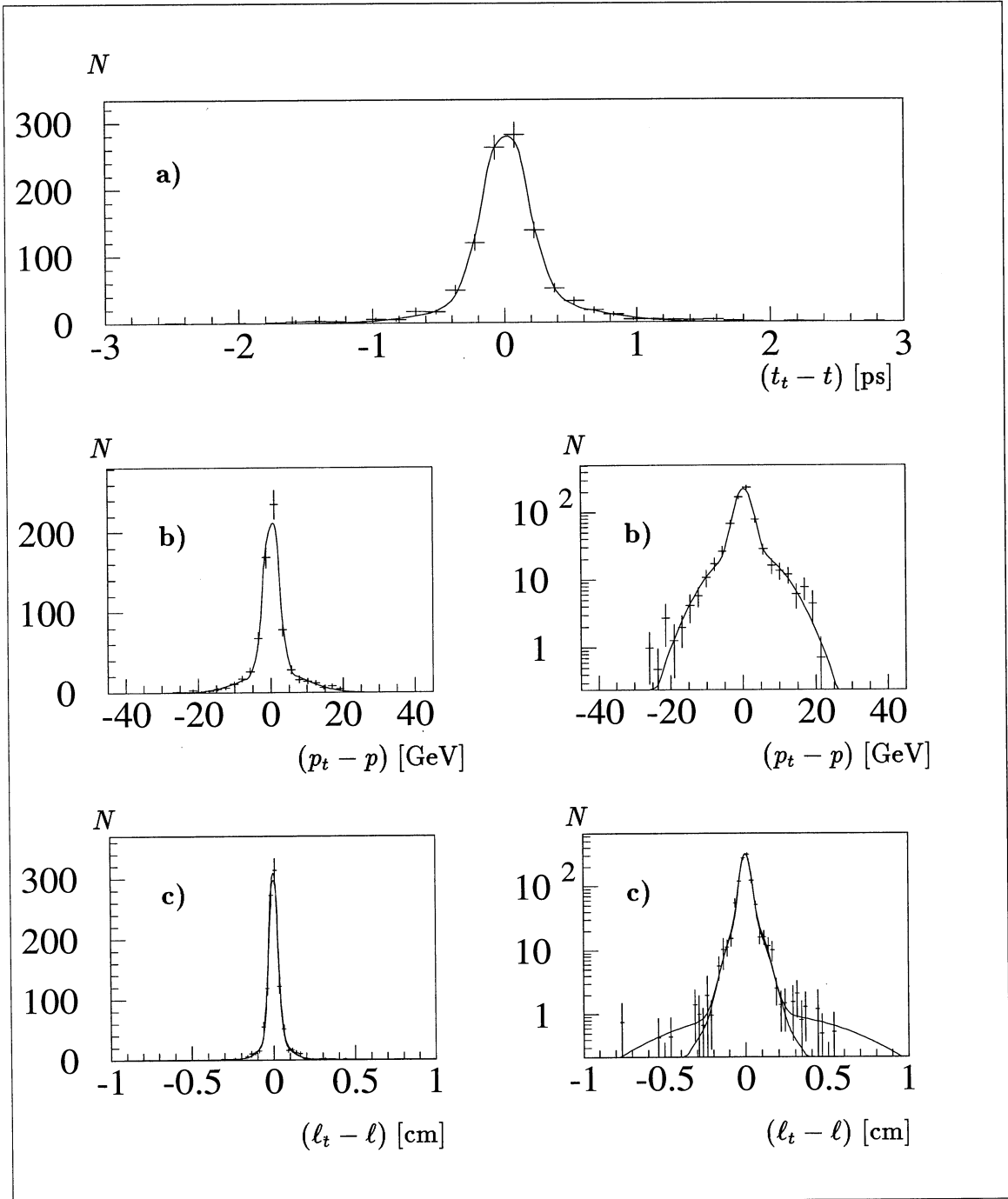
2

Figure 1: Time (a), momentum (b) and decay length (c) resolution from Monte Carlo events.

- **B^0 flight direction:**
  The B^0 flight direction $\vec{\ell}_B$ was obtained by using the jet which contains the fast pion π_B^+. The jet (YCUT=0.008) was required to lie in the central part of the detector:

$$|\cos\vartheta_{jet}| \; < \; 0.7 \tag{7}$$

The jet direction has to agree with the B^0 flight direction from the vertices

$$\chi^2_{dir} \; < \; 4 \tag{8}$$

See equation 5 for the definition of χ^2_{dir}.

- **B^0 lifetime :**
  In this study candidates with a proper time

$$20\text{ ps} > t > 1\text{ ps} \tag{9}$$

were used. Below 1 ps u, d, s and c background events are dominant.

- **B^0 kinematics:**
  The approximation of the B^0 momentum was determined following the technique described above. $\pi_B^+ \pi_D^-$ candidates fulfilling

$$30\text{ GeV} < \quad |\vec{p}_B| \quad < 45\text{ GeV} \tag{10}$$
$$|\cos\vartheta^*_{B,\pi_B^\pm}| \; < 0.8 \tag{11}$$

are accepted. The requirement on the B^0 decay angle $\vartheta_{B,\pi_B^\pm}$ is similar to a p_t cut but does not effect the $\pi^+\pi^-$ mass distribution.

- **Comparison of B^0 flight direction:**
  The B^0 flight direction has been determined independently by reconstructing the B^0 momentum $\vec{p}_B$ and from the measurement of the decay length $\vec{\ell}_B$. The angle α between these two directions was required to be smaller than:

$$\alpha \; < \; 0.025 \tag{12}$$

- **$B^+ \to \pi^+ X D^{**0}$ suppression:**
  Applying the cuts above the expected background from B^+ decays is $N(B^+ \to D^{*-})/N(B^{+,0} \to D^{*-}) = 0.17$ according to a Monte Carlo simulation. To reduce B^+ background

$$B^+ \to \pi^+\pi^+ X D^{*-} \tag{13}$$

events with an additional pion from the secondary vertex were rejected. The selection criteria fro these events are:

- dE/dx of the additional pion: $\chi^2_\pi < 4$, $\chi^2_K > 1$.

– the pion comes from the B vertex:

$$prob^{impact\ parameter}_{main\ vertex} < 5\% \tag{14}$$

$$prob^{impact\ parameter}_{\pi\pi\ vertex} > 5\% \tag{15}$$

– The B^+ flight direction can be calculated in the same way as for a B^0 candidate using $M_{XD^0} = M_{D^0}$ in formula 2 and replacing $M_{\pi_B\pi_D}$ by the mass of the three measured pions. The angle α was required to be smaller than $\alpha < 0.02$.

This selection has an efficiency of 60 % for $B^+ \to \pi^+\pi^+XD^{*-}$ events. Due to the rejection of these events only 20% of the B^0 decays are lost. The $\pi^+\pi^-$ mass spectrum of the rejected events is given in figure 3.

The $\pi^+\pi^-$ mass distribution for all combinations which pass the selection is given in figure 2. It shows an enhancement at small masses. In table 1 the observation is compared with the Monte Carlo expectation.

2.4 Background

For the lifetime measurement events in the mass range $m_{\pi\pi} = 1 - 1.5$ GeV will be used. This sample consists of three parts:

- $B \to \pi^+_B D^{*-}X$ **events**
  These can be B^0 or B^+ decays.

  – B^0 **Signal.**
    The expected composition of the $B^0 \to \pi^+_B XD^{*-} \to \pi^+_B X(\pi^-_D\overline{D}^0)_{D^{*-}}$ sample is given in table 1.

  – B^+ **background.**
    Background events of the type $B^+ \to \pi^+_B XD^{*-} \to \pi^+_B X(\pi^-_D\overline{D}^0)_{D^{*-}}$ are expected to come mainly from two body decays with a D^{**} [1]. The amount of background relative to the B^0 signal was estimated from the Monte Carlo simulation to be $B^+/(B^+ + B^0) = (8.3^{+2.3}_{-2.4})\%$. This ratio can be determined as well from a fit to the $\pi^+_B\pi^-_D$ mass spectrum or from the rejected events with an additional pion from the secondary vertex (figure 3). The obtained ratios (table 1) are in good agreement with each other. To take into account uncertainties in the D^{**} production rates an additional 50% systematic error was added:

$$\frac{B^+}{B^+ + B^0} = (8.3^{+2.3}_{-2.4} \pm 4.1)\% \tag{16}$$

- **Combinatorial background.**
  The combinatorial background was estimated from the Monte Carlo simulation. The $\pi^+\pi^-$ mass spectrum for this background is shown in figure 2. Above
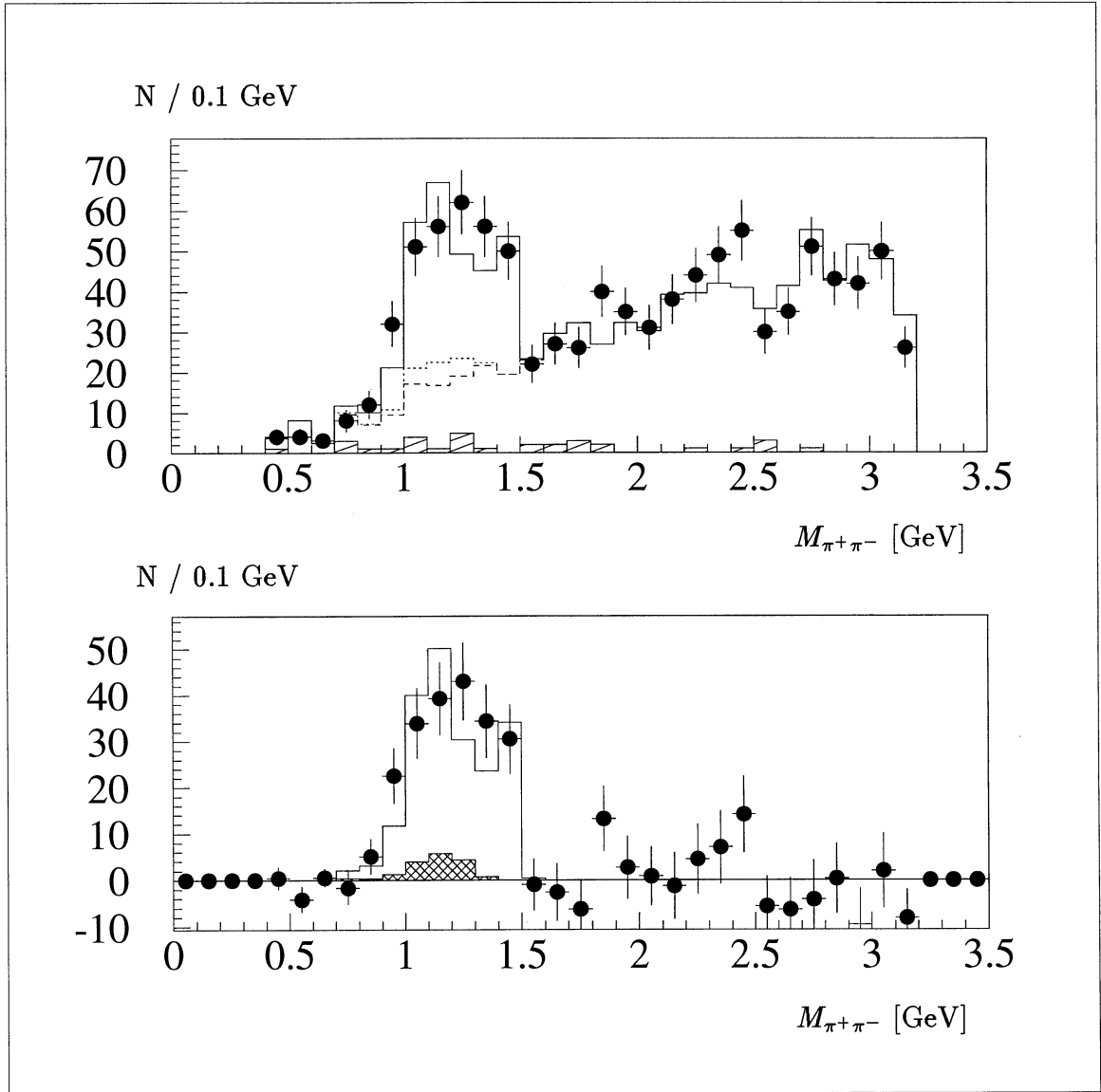
Figure 2: $\pi_B^+\pi_D^-$ mass distributions. Shown are in figure **a)** the data (with error bars) and the Monte Carlo simulation (histograms). In the histograms the contributions from $q\bar{q}$ background, $b\bar{b}$ background, $B^+ \to \pi_B^+ X D^{*-}$ and the $B^0 \to \pi_B^+ X D^{*-}$ signal are added. The dots with error bars in figure **b)** are the data after subtraction of the $q\bar{q}$ and $b\bar{b}$ background. The histograms are the predictions for $B^+ \to \pi_B^+ X D^{*-}$ and the sum of $B^0, B^+ \to \pi_B^+ X D^{*-}$ decays.

6
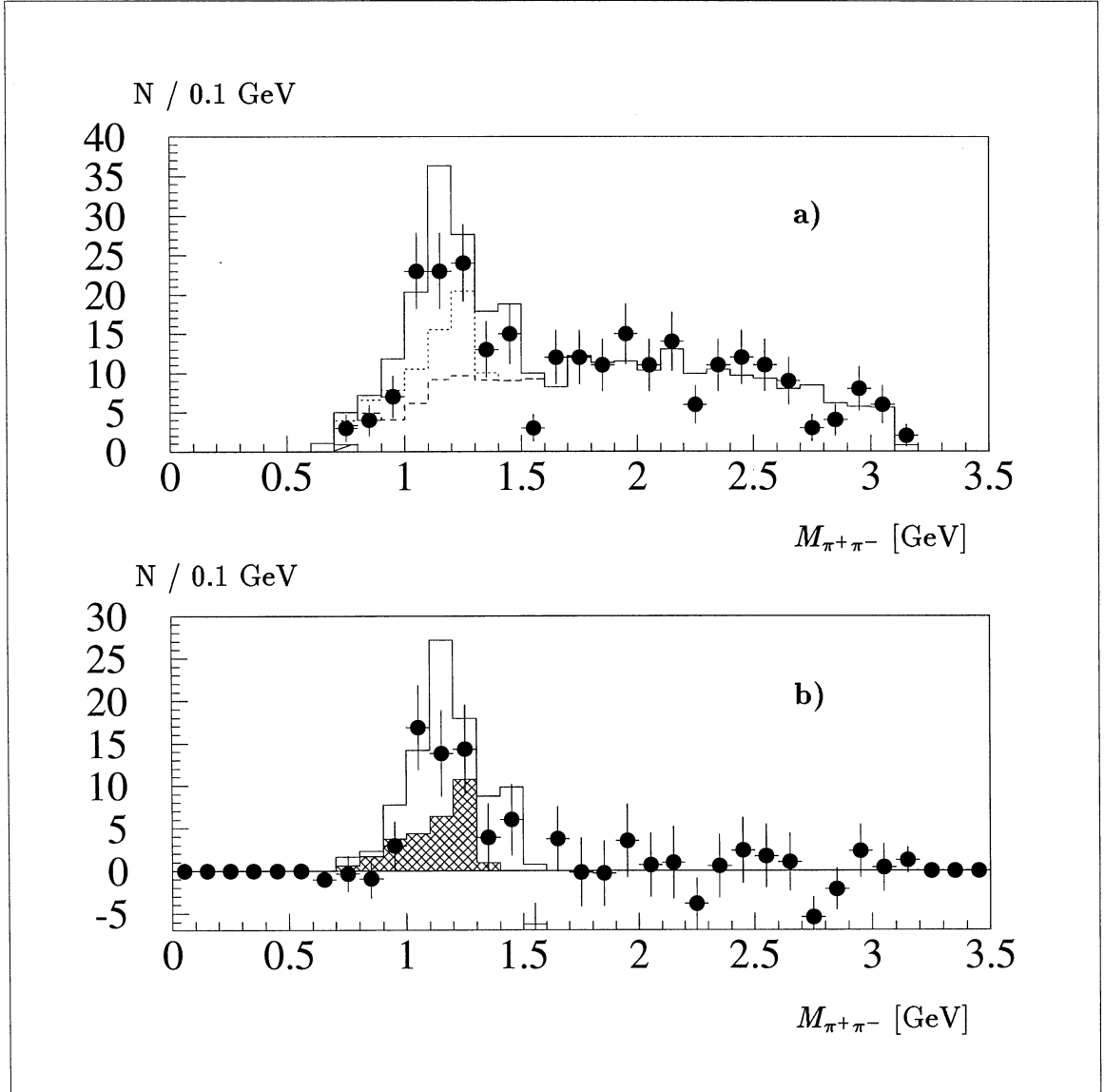
Figure 3: $\pi_B^+\pi_D^-$ mass distributions for the B^+ candidates. Shown are in figure a) the data (with error bars) and the Monte Carlo simulation (histograms). In the histograms the contributions from $q\bar{q}$ background, $b\bar{b}$ background, $B^+ \rightarrow \pi_B^+ X D^{*-}$ and the $B^0 \rightarrow \pi_B^+ X D^{*-}$ signal are added. The dots with error bars in figure b) are the data after subtraction of the $q\bar{q}$ and $b\bar{b}$ background. The histograms are the predictions for $B^+ \rightarrow \pi_B^+ X D^{*-}$ and the sum of $B^0, B^+ \rightarrow \pi_B^+ X D^{*-}$ decays.

	# events	systematic errors $\epsilon_b =$ $(32 \pm 17) \cdot 10^{-3}$	scaling	total
data	275 ± 16.6			
$b\bar{b}$ background (MC)	83.4 ± 5.2		± 6.5	
$q\bar{q}$ background (MC)	10.6 ± 3.2		± 0.8	
excess	181.0 ± 17.7	$\pm^{1.5}_{0.7}$	± 7.3	181.0 ± 19.2

MC expectations	# events	systematic errors $\epsilon_b =$ $(32 \pm 17) \cdot 10^{-3}$	BR	total
$B^0 \to \pi^+ D^{*-}$	57.3 ± 3.7		± 8.4	
$B^0 \to \rho^+ D^{*-}$	44.5 ± 6.0		± 9.3	
$B^0 \to (\pi^+, \rho^+)(\pi^0 D^{*-})_{D**}$	20.8 ± 2.7		± 6.2	
$B^0 \to X_{rest} D^{*-}$	40.7 ± 4.4			
Sum B^0	163.3 ± 8.7	$\pm^{3.7}_{4.3}$	± 14.0	$163.3\pm^{16.9}_{17.0}$
$B^+ \to \pi^+(\pi^+ D^{*-})_{D**}$	10.2 ± 1.6		± 3.1	
$B^+ \to \rho^+(\pi^+ D^{*-})_{D**}$	2.2 ± 1.2		± 0.7	
$B^+ \to X_{rest} D^{*-}$	2.3 ± 1.0			
Sum B^+	14.7 ± 2.2	$\pm^{0.0}_{1.1}$	± 3.2	$14.7\pm^{3.9}_{4.0}$
Sum B^0, B^+	178.0 ± 9.0	$\pm^{1.4}_{4.4}$	± 14.4	$178.0\pm^{17.0}_{17.5}$
Ratio B^+/B (MC)				$(8.3\pm^{2.3}_{2.4})\%$
Ratio B^+/B (fit to $M_{\pi^+\pi^-}$)				$(12 \pm 22)\%$
Ratio B^+/B (B^+ selection)				$(3.2 \pm 5.6)\%$

Table 1: Observed and expected number of events in the signal mass region $M_{\pi\pi} = 1 - 1.5 \ GeV$.

$m_{\pi\pi} > 1.5$ GeV the B^0 signal and B^+ background cannot contribute due to the decay kinematics. Therefore the number of events with $m_{\pi\pi} > 1.5$ GeV can be used to normalize the Monte Carlo spectrum. The number of background events are then obtained from an extrapolation to the signal mass region $m_{\pi\pi} = 1 - 1.5$ GeV. This leads to 94.0 ± 9.6 background events. A systematic error of 7.9% is added (see section 3.1.3).

3 The B^0 Lifetime Measurement

3.1 Signal and Background Time Distributions

For an unbinned maximum likelihood fit the time distributions must be known in an analytical form. Three functions for the three components are needed.

3.1.1 The B^0 signal events

The distribution of the measured time t is given by:

$$f_s(t) = a_s \int_{p_{min}}^{p_{max}} dp \int dp_t \int d\ell_t \underbrace{R^\ell(\ell, \ell_t)\, R^p(p, p_t)}_{\substack{\text{resolution} \\ \text{functions}}} \underbrace{\epsilon(p_t, \ell_t)}_{\text{efficiency}} \underbrace{g(p_t)}_{\substack{\text{momentum} \\ \text{spectrum}}} \underbrace{\frac{1}{\tau} e^{-t_t/\tau}}_{\substack{\text{decay} \\ \text{function}}}$$

$$= a_s \frac{c}{M_B} \int dt_t\, \frac{1}{\tau}\, e^{-t_t/\tau} \underbrace{\int dp_t\; p_t\; \epsilon(p_t, \ell_t)\, g(p_t) \int_{p_{min}}^{p_{max}} dp\; R^\ell(\ell, \ell_t)\, R^p(p, p_t)}_{G(t, t_t)} \qquad (17)$$

The integration over the measured momentum p covers the range $p \in [p_{min}, p_{max}] = [30\ GeV, 45\ GeV]$. The momentum and decay length resolution are obtained from the Monte Carlo. Parametrizations with two gaussians for the momentum resolution and three gaussians for the decay length were used (figure 1). The efficiency (figure 4) is assumed to factorize $\epsilon(p_t, l_t) = \epsilon(p_t)\epsilon(l_t)$. The spectrum of the true momentum p_t comes from Monte Carlo using the measured fragmentation parameter $\epsilon_b = 0.0032$ [2]. a_s is a normalization function to guarantee $\int_{t_{min}}^{t_{max}} dt\, f(t) = 1$ for the time region $t \in [t_{min}, t_{max}] = [1\ ps, 20\ ps]$.

3.1.2 Time Distribution for the B^+ Background

This background is the smallest of the three contributions. The corresponding time distribution can be approximated by a simple exponential with an effective B^+ lifetime.

$$f_+(t) = \exp(t, \tau_+^{eff}) \qquad (18)$$

$\exp(t, \tau)$ is a normalized exponential:

$$\exp(t, \tau) = \frac{1}{\tau} \cdot \left(e^{-t_{min}/\tau} - e^{-t_{max}/\tau} \right)^{-1} \cdot e^{-t/\tau} \qquad (19)$$

The effective lifetime $\tau_+^{eff} = 1.05 \pm 0.17\ ps$ is obtained from Monte Carlo using the world average B^+ lifetime $\tau_+ = 1.67\ ps$ [3].

3.1.3 Time Distribution for the Combinatorial B^+ Background

For the combinatorial background a sum of two normalized exponentials was used:

$$f_b(t) = r_b \cdot \exp(t, \tau_{b1}) + (1 - r_b)\exp(t, \tau_{b2}) \qquad (20)$$

The parameters r_b, τ_{b1} and τ_{b2} are free in the fit but restricted by using data events to describe the background.

One method to describe the background is to use the wrong charge combination, $\pi_B^\pm \pi_D^\pm$, applying the same selection criteria as for the $\pi_B^\pm \pi_D^-$ signal candidates. Due to the large difference in the momentum between the two pions (one is assumed to come directly from the B^0 while the second is the slow pion from the D^{*-} decay) the charge
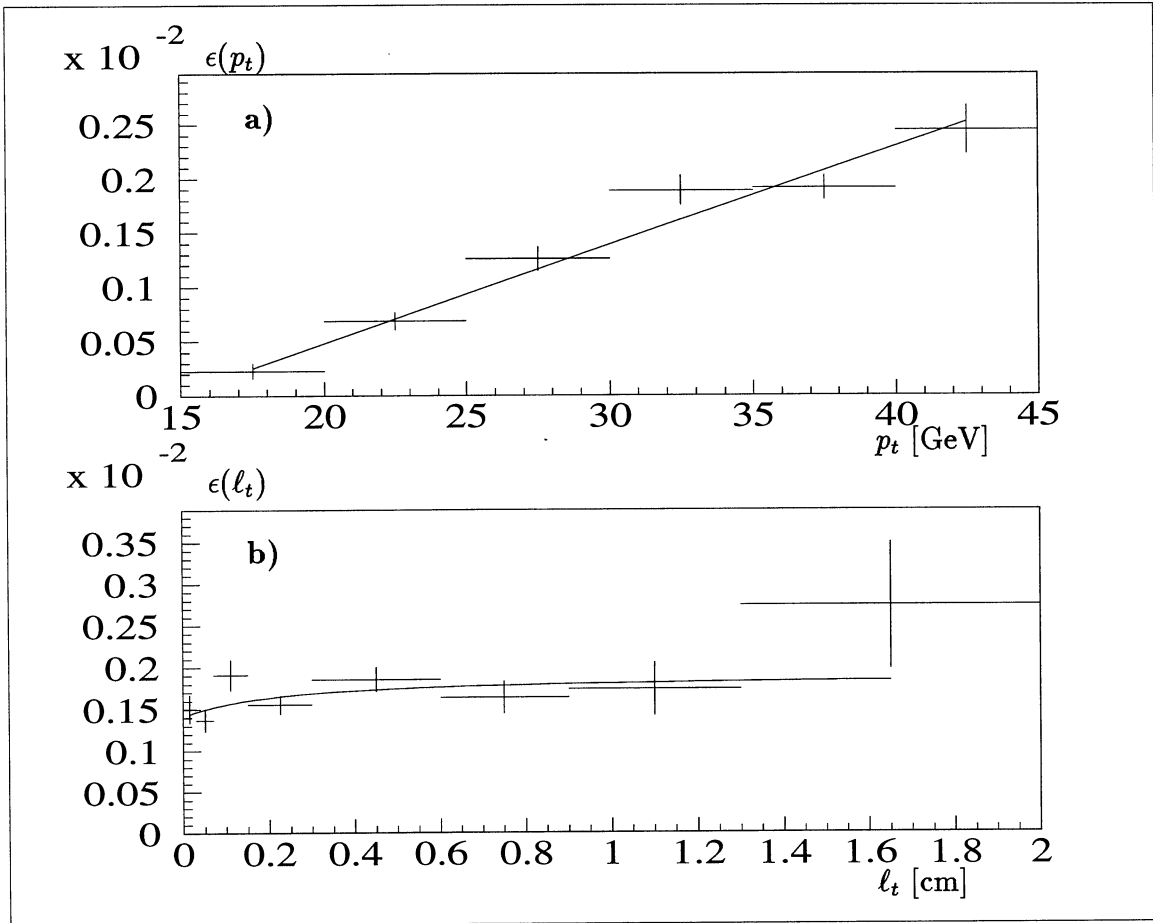
9

Figure 4: Efficiency in Monte Carlo events.

correlation is expected to be small for the background. The $\pi_B^{\pm}\pi_D^{\pm}$ mass spectrum for the wrong charge combinations is shown in figure 5. A good agreement is found between data and Monte Carlo with no enhancement in the signal mass region.

In addition to the fact that the charge correlation is small, also the correlation between the pion momenta transverse to the jet axis is small for background events. Slow pions are distributed almost symmetric around the jet axis. A second sample was obtained selecting events with $\pi_B^+\pi_D^-$ combinations by first rotating the π_D^- around the jet axis in such a way that the difference in momentum before and after the rotation is 200 MeV. The rotation angle β which can be either positive or negative was restricted to $|\beta| \leq 90^o$. This rotation is large enough to destroy the kinematic correlation for signal events. This sample is called π_B^+ $rot(\pi_D^-)$ sample.

A third sample, $\pi_B^{\pm}$ $rot(\pi_D^{\pm})$, was selected by using wrong charge combinations together with a rotation around the jet axis.

The $\pi\pi$ mass distributions for the three samples are shown in figure 5. For the final

fit all three samples were used together.[1] The assumption that the time distribution of the background sample describes the real background can be tested for the signal mass region using Monte Carlo and for the mass region $m_{\pi\pi} > 1.5$ GeV where no signal events can contribute (figure 6).

In addition these background samples were used to check the determination of the amount of combinatorial background. Normalizing the Monte Carlo background spectrum to the data in the mass region $m_{\pi\pi} > 1.5$ GeV gives a prediction for the expected number of events in the data in the mass range $m_{\pi\pi} = 1 - 1.5$ GeV of 292 ± 18 events. In the data 318 events were observed. The statistical error of $\frac{\sqrt{18^2 + 318}}{318} = 7.9\%$ was taken as a systematic error on the number of combinatorial background events.

4 The Lifetime Fit

The B^0 lifetime was obtained from an unbinned maximum likelihood fit. The fit parameters are:

τ_0	: B^0 lifetime
N_s	: Number of events $B^0 \to \pi_B^+ X (D^0 \pi_D^-)_{D^*}$, $B^+ \to \pi_B^+ X (D^0 \pi_D^-)_{D^*}$
N_b	: Number of background events. A constraint on this parameter comes from chapter one: $< N_b >= 94.0 \pm 9.6$.
r_+	: relative amount of B^+ background, constrained to $< r_+ >= 8.3 \pm 4.8\%$.
$r_b, \tau_{b1}, \tau_{b2}$	: parameters to describe the background time spectrum.
τ_+^{eff}	: the effective lifetime for the B^+ background ($< \tau_+^{eff} >= 1.01 \pm 0.17$ ps).

The Likelihood function is a product for the signal sample and the background sample:

$$\mathcal{L} = \mathcal{L}^{signal}(\tau; \ r_+, N_s, N_b, r_b, \tau_{b1}, \tau_{b2}, \tau_+^{eff}) \cdot \mathcal{L}^{backg}(r_b, \tau_{b1}, \tau_{b2}) \tag{21}$$

The likelihood for the signal part is given by:

$$\mathcal{L}^{signal} = e^{-\frac{(N_b - <N_b>)^2}{2\sigma_{N_b}^2}} \cdot e^{-\frac{(r_+ - <r_+>)^2}{2\sigma_{r+}^2}} e^{-\frac{(\tau_+ - <\tau+>)^2}{2\sigma_{\tau+}^2}} e^{-N_s - N_b} \cdot \prod_i^{\substack{signal \\ sample}} \mathcal{P}_i \tag{22}$$

with

$$\mathcal{P} = N_s [(1 - r_+)f_s + r_+ f_+] + N_b f_b \tag{23}$$

The functions f_s, f_b and f_+ were already defined in the previous section. The parameters for the background function are mainly determined from the likelihood function for the background sample:

$$\mathcal{L}^{backg} = \prod_i^{\substack{background \\ sample}} f_{b,i} \tag{24}$$
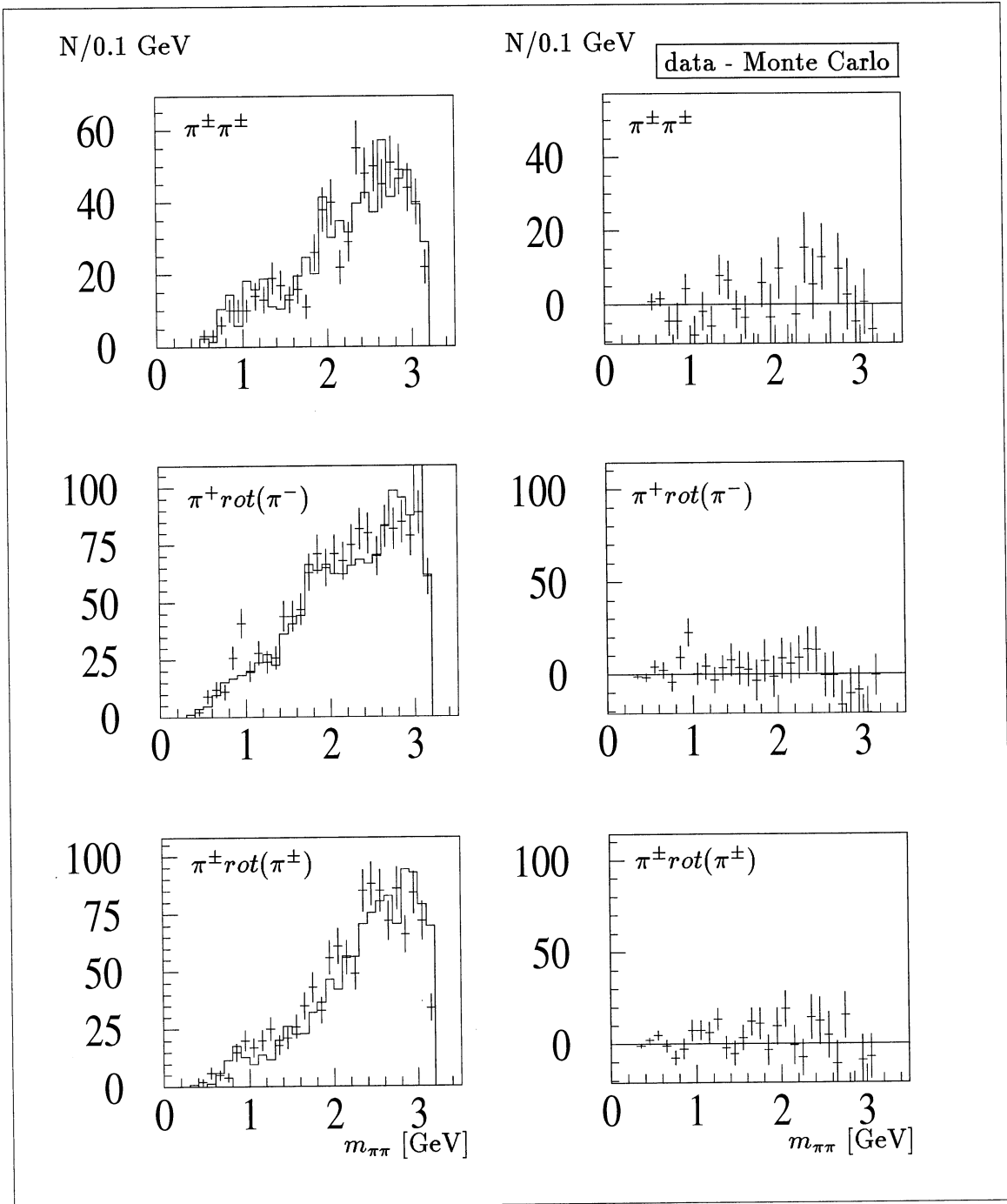
---

[1]Double entries were rejected.

Figure 5: Comparison of the $\pi\pi$ mass distributions for data and Monte Carlo background samples.
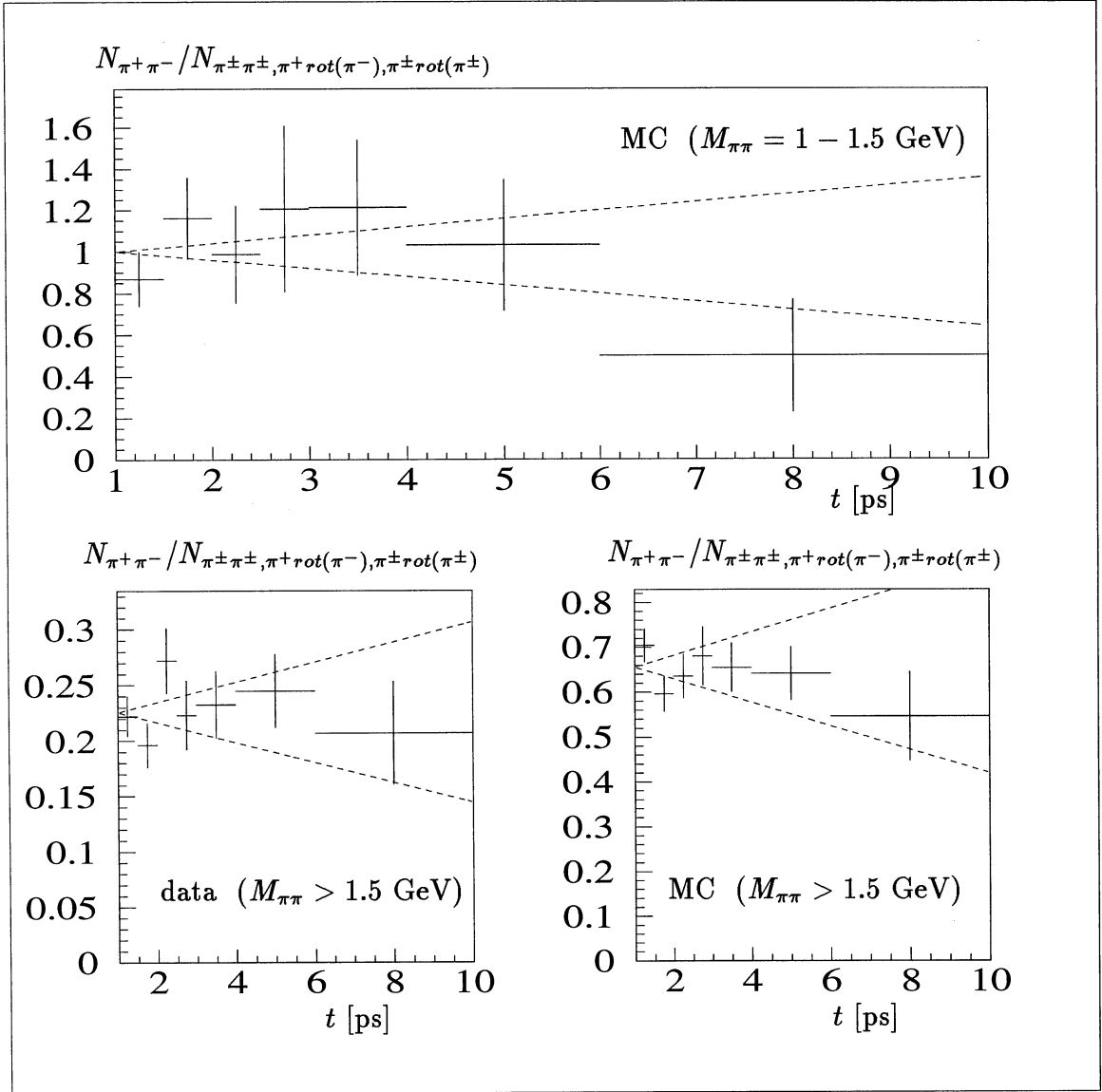
Figure 6: Ratio of background events in the $\pi^+\pi^-$ sample and events in the background sample. The upper figure shows the ratio for Monte Carlo events in the signal mass range. In addition the ratio is given in the mass range above 1.5 GeV for Monte Carlo events and data. The dashed lines indicates the uncertainty for this ratio which was taken into account in the systematic error.

The result of the fit is shown in figure 7. The values obtained for the fit parameters are listed in table 2. The lifetime was determined to be

$$\tau_{B^0} = 1.50 \; ^{+0.17}_{-0.15} \; ^{+0.08}_{-0.05} \; ps \tag{25}$$

The second error is the systematic error. The contributions to this error can be found in table 3 and were obtained in the following way:

- **Background time distribution**
  The test that the background sample shows the same time behavior as the real background (figure 6) is limited by statistics. The distributions in figure 6 are all compatible with a constant ratio. The function f_b was modified for the signal likelihood $f_b \to a(1 + b \cdot \ell_t) \cdot f_b$ with a slope $b = \pm 0.04$ as shown in figure 6.

- **Background function**
  The background time distribution $f_b(t)$ was parametrized by only one exponential.

- **Momentum and decay length resolution**

  - The reconstructed decay length was shifted by $\pm 50 \; \mu m$.

  - The resolution function R^ℓ was parametrized with two gaussian instead of three.

- **Efficiency**

  - The statistical error of the efficiency functions was taken into account.

  - $\epsilon(\ell_t)$ was parametrized by a function $\epsilon(\ell_t) = a \arctan(b \cdot \ell_t)$ instead of $\epsilon(\ell_t) = a(1 + b/(1 + c \cdot \ell_t))$.

  - The effect of the signal composition was studied by enhancing or reducing the $B^0\pi^+, \rho^+ D^{*-}$ contributions by a factor of 2. No polarization was assumed in a second test.

- **B^+ lifetime**
  Varying the B^+ lifetime $\tau_{B+} = 1.67 \pm 0.08 \; ps$ [3] within the error $\pm 0.08 \; ps$ changes the B^0 lifetime by $^{-0.005}_{+0.002} \; ps$.

- **Fragmentation function**
  The fragmentation parameter $\epsilon_b = 0.0032 \pm 0.0017$ was varied within the error.

- **Integration of $G(t, t_t)$**
  The integration of $G(t, t_t)$ was done numerically. The number of points used in the integration was reduced by a factor of 27.

The systematic uncertainties on the amount of background events is includes in the definition of the likelihood function and therefore part of the statistical error.
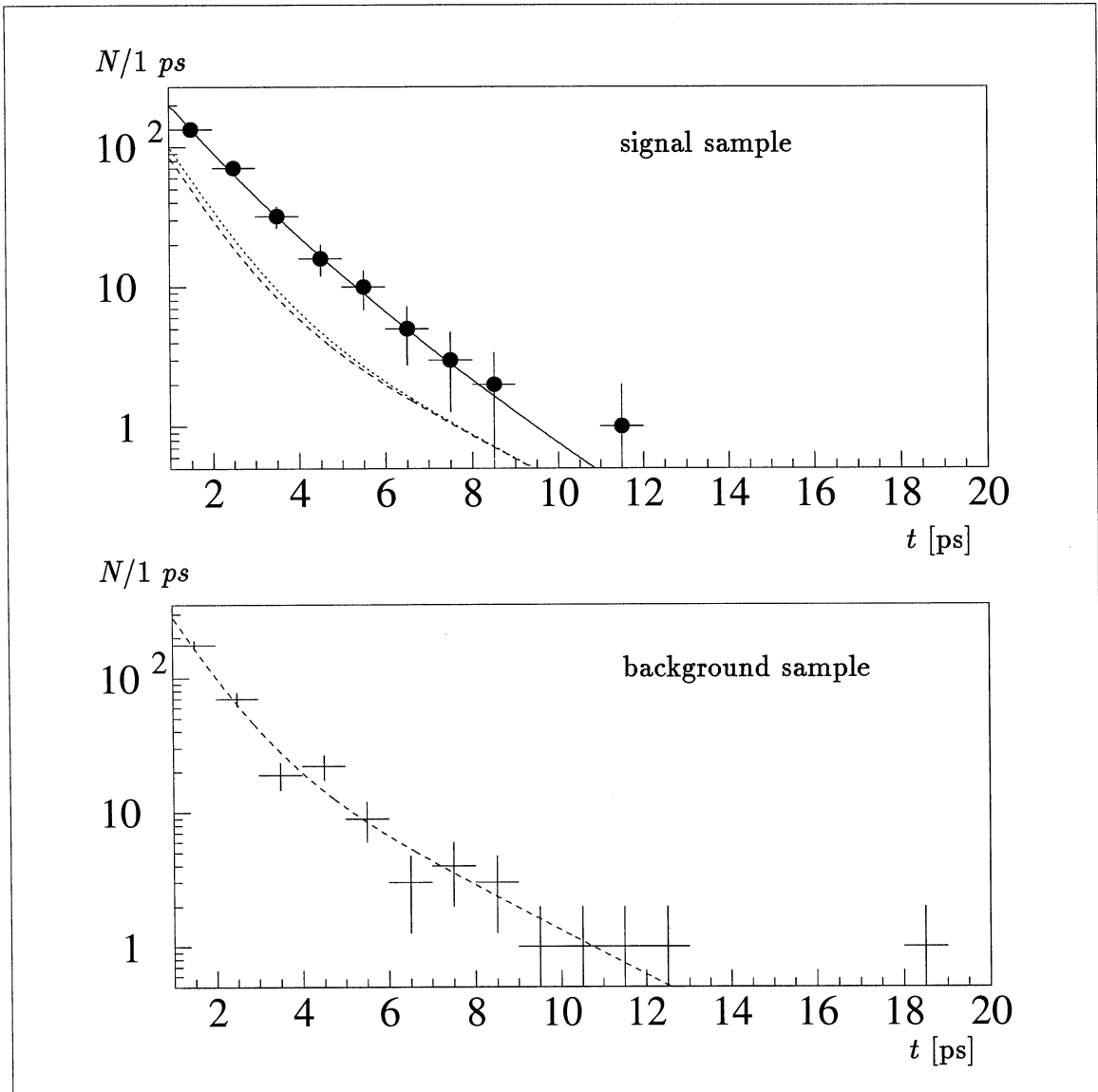
Figure 7: Fit results for the signal and the background sample. For the signal sample the combinatorial background contribution (dashed) and the total background (dotted) including $B^+ \to \pi^+ X D^{*-}$ decays are plotted as well.

15

		correlation coefficients							
		τ	N_s	N_b	r_b	τ_{b1}	τ_{b2}	r_+	$\tau+$
τ	$= 1.50^{+0.17}_{-0.15}$	1.000	-0.056	0.055	0.132	0.054	0.041	0.166	-0.076
N_s	$= 183 \pm 19$		1.000	-0.490	-0.007	-0.031	0.015	0.006	-0.005
N_b	$= 92.9 \pm 9.5$			1.000	0.007	0.031	-0.015	-0.006	0.005
r_b	$= 0.66^{+0.16}_{-0.17}$				1.000	0.886	0.892	0.004	-0.008
τ_{b1}	$= 0.84^{+0.19}_{-0.18}$ ps					1.000	0.757	0.013	-0.016
τ_{b2}	$= 2.64^{+0.91}_{-0.49}$ ps						1.000	0.000	-0.003
r_+	$= 0.080 \pm 0.048$							1.000	0.041
τ_+^{eff}	$= 1.02 \pm 0.17$ ps								1.00

Table 2: Fit result.

systematic error	
background time distribution	$^{+0.057}_{-0.044}$ ps
background function	± 0.011 ps
momentum and decay length resolution	± 0.024 ps
efficiency (MC statistic)	$^{+0.037}_{-0.020}$ ps
efficiency (ϵ_ℓ, signal composition)	± 0.019 ps
B^+ lifetime	$^{+0.002}_{-0.005}$ ps
fragmentation function	$^{+0.006}_{-0.008}$ ps
integration of $G(t, t_t)$	± 0.003 ps
sum	$^{+0.076}_{-0.059}$ ps

Table 3: Systematic uncertainties.

5 Conclusions

Hadronic decays $B^0 \to \pi_B^+ X D^{*-} \to \pi_B^+ X (\pi_D^- \overline{D}^0)_{D^*}$ were partially reconstructed from two charged pions $\pi_B^+ \pi_D^-$. 166 ± 13 decays were observed in the 1991-1994 data. 62% percent of the decays are expected to come from the two body reactions $B^0 \to \pi^+ (\rho^+) D^{*-}$. From these events the B^0 lifetime was measured to be:

$$\tau_{B^0} = 1.50 \; ^{+0.17}_{-0.15} \; ^{+0.08}_{-0.06} \; ps$$

References

[1] T. Oest , *A Measurement of the B^0 Lifetime from Partial Reconstructed Hadronic B^0 Decays*, ALEPH 94-178, November 1994.

[2] D. Buskulic *et al* (ALEPH Collaboration), Z. Phys. **C62** (1994) 179.

[3] R. Forty , CERN-PPE/94-144.